JACS
JOURNAL OF THE AMERICAN CHEMICAL SOCIETY

Communication

Multicomponent Pt-based Zigzag Nanowires as Selectivity Controllers for Selective Hydrogenation Reactions

Shuxing Bai, Lingzheng Bu, Qi Shao, Xing Zhu, and Xiaoqing Huang

J. Am. Chem. Soc., **Just Accepted Manuscript** • DOI: 10.1021/jacs.8b03862 • Publication Date (Web): 20 Jun 2018

Just Accepted

ACS Publications

is published by the American Chemical Society. 1155 Sixteenth Street N.W., Washington, DC 20036

Multicomponent Pt-based Zigzag Nanowires as Selectivity Controllers for Selective Hydrogenation Reactions

Shuxing Bai,[†] Lingzheng Bu,[†] Qi Shao,[†] Xing Zhu,[‡] and Xiaoqing Huang[*†]

[†]College of Chemistry, Chemical Engineering and Materials Science, Soochow University, Jiangsu, 215123, China.

[‡]Testing & Analysis Center, Soochow University, Jiangsu, 215123, China.

Supporting Information Placeholder

ABSTRACT: The selective hydrogenation of α, β-unsaturated aldehyde is an extremely important transformation, while developing efficient catalysts with desirable selectivity to highly value-added products is challenging, mainly due to the coexistence of two conjugated unsaturated functional groups. Herein, we report that a series of Pt-based zigzag nanowires (ZNWs) can be adopted as selectivity controllers for α, β-unsaturated aldehyde hydrogenation, where the excellent unsaturated alcohol (UOL) selectivity (> 95%) and high saturated aldehyde (SA) selectivity (> 94%) are achieved on PtFe ZNWs and PtFeNi ZNWs+$AlCl_3$, respectively. The excellent UOL selectivity of PtFe ZNWs is attributed to the lower electron density of the surface Pt atoms, while the high SA selectivity of PtFeNi ZNWs+$AlCl_3$ is due to synergy between PtFeNi ZNWs and $AlCl_3$, highlighting the importance of Pt-based NWs with precisely controlled surface and composition for catalysis and beyond.

The selective hydrogenation of α, β-unsaturated aldehyde to unsaturated alcohol (UOL) or saturated aldehyde (SA) is a vital process in petrochemical, biological and chemical industries.[1,2] Nevertheless, it is a very complex process since α, β-unsaturated aldehyde has two unsaturated functional and conjugated alkene bond (C=C) and carbonyl (C=O) groups.[3,4] In general, owing to thermodynamic favoring of the C=C hydrogenation over the C=O hydrogenation, it is extremely difficult to achieve high selectivity of C=O hydrogenation.[5,6] Moreover, when there is a bulky group or an extra unsaturated group conjugated with C=C, such as cinnamaldehyde (CAL) and furfural, high selectivity for C=C hydrogenation also becomes challenging.[7]

Many researches about selective hydrogenation catalysts for α, β-unsaturated aldehyde have been primarily centered on platinum (Pt)-based catalysts, owing to their excellent activity, while poor selectivity of pure Pt restricts their practical applications.[8,9] The conventional methods to improve the selectivity of UOL or SA are modifying the undesirable active sites by surface ligands, thiolate, oxide or metal-organic frameworks,[1,3,6,10] while the selectivity improvement is often accompanied by sacrificing activity.[1,6] Pt-based alloy catalysts become the focus of study, which usually offer the synergistic effects to obtain high selectivity to desired products.[11-14] Alloying 3d transition metal with Pt can particularly alters the *d*-band center of surface Pt, which has been proved to enhance the performance of targeted reaction.[15-20] Although high UOL and SA selectivity can be realized separately,[21-24] the simultaneous realization of high UOL and SA selectivity remains a great challenge.

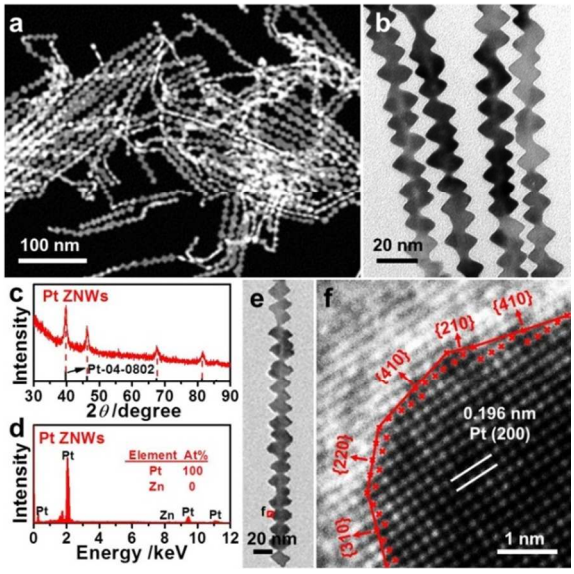

Figure 1. (a) HAADF-STEM image, (b, e) TEM images, (c) XRD, (d) SEM-EDX, and (f) HRTEM image of Pt ZNWs.

Herein, we show that Pt-based zigzag nanowires (ZNWs) can be serviced as the selectivity controllers for α, β-unsaturated aldehyde hydrogenation. While the PtFe ZNWs can represent excellent UOL selectivity, the PtFeNi ZNWs exhibit promising SA selectivity by introducing $AlCl_3$. Significantly, the excellent activity of Pt-based ZNWs is well preserved. The excellent C=O hydrogenation selectivity of PtFe ZNWs is due to the lower electron density of the surface Pt atoms, and the high C=C hydrogenation selectivity of PtFeNi ZNWs+$AlCl_3$, in which PtFeNi ZNWs provide highly active sites and AlCl3 is used as aldehyde protector.

The Pt-based ZNWs were made through a wet-chemical process. Taken Pt ZNWs as example, platinum (II) acetylacetonate ($Pt(acac)_2$), zinc (II) acetylacetonate ($Zn(acac)_2$), ribose and cetyltrimethyl ammonium chloride (CTAC) were dissolved in the mixed solvent of oleylamine (OAm) and diphenyl ether (DPE). The solution was gradually heated to 160 ºC and maintained for 5 h. The Pt ZNWs are uniform with the diameter of ~12 nm, as confirmed by the high angle

annular dark field scanning transmission electron microscopy (HAADF-STEM, **Figure 1a**) and TEM (**Figure 1b**) images. Notably, the surface of these ZNWs represent the zigzag borders.[25,26] The X-ray diffraction (XRD) pattern (**Figure 1c**) of Pt ZNWs is assigned to face-centered cubic (*fcc*) phase of Pt (PDF No. 04-0802). The elemental compositions are measured by scanning electron microscopy energy-dispersive X-ray spectroscopy (SEM-EDX, **Figure 1d**), in which the Pt/Zn atomic ratio is approaching to 100%/0%. Pt ZNWs can only be obtained by introducing $Zn(acac)_2$ (**Figure S1**). The 0.196 nm lattice spacing of Pt ZNWs corresponds to the (200) facet of Pt, as confirmed by high-resolution TEM image (HRTEM, **Figure 1e-f**), in which the steps and high-index facets ({410}, {310}, {220}, and {210}) can be readily observed.[27]

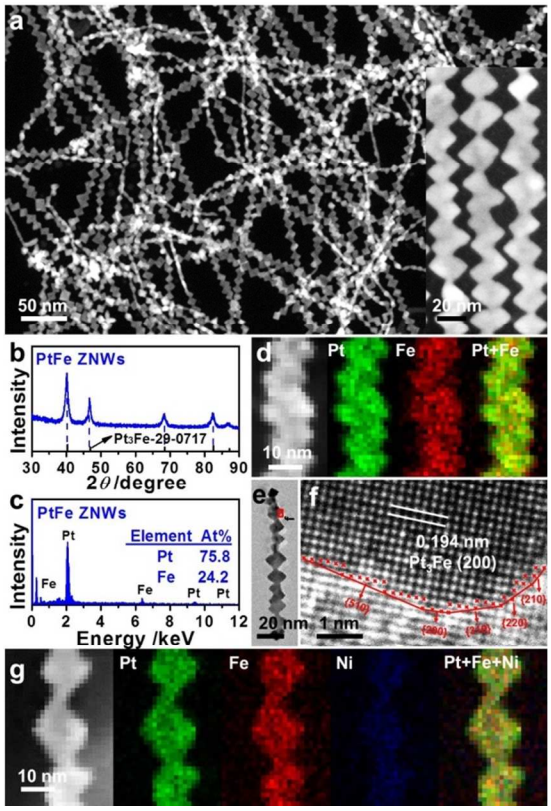

Figure 2. (a) HAADF-STEM image, (b) XRD, (c) SEM-EDX, (d) HAADF-STEM image and elemental mappings, (e) TEM image and (f) HRTEM image of PtFe ZNWs. (g) HAADF-STEM elemental mappings of PtFeNi ZNWs.

A synthetic strategy was also developed for PtFe ZNWs (Supporting information for details). The product was characterized by HAADF-STEM (**Figure 2a**), where 1D nanostructures with zigzag borders, average diameter of 12 nm and length up to micrometers are clearly observed. The XRD pattern of PtFe ZNWs (**Figure 2b**) matches well with that of *fcc* Pt_3Fe (PDF No. 29-0717).[28] The Pt/Fe atomic ratio of the ZNWs is 75.8%/24.2%, as determined by SEM-EDX (**Figure 2c**). Although the PtFe ZNWs have rough surface and zigzag border, Pt and Fe distribute evenly in the whole ZNWs (**Figure 2d**). As shown in **Figure 2e-f**, the 0.194 nm lattice spacing is assigned to the (200) facet of *fcc* Pt_3Fe and many steps and high-index facets are also observed.

The trimetallic PtFeNi ZNWs can also be synthesized by introducing additional Ni precursor into the preparation of PtFe ZNWs (**Figure S2**).[19] The ZNWs were confirmed by HAADF-STEM and TEM images (**Figure S2a-b**). The diffraction peaks of PtFeNi ZNWs (**Figure S2c**) can be assigned to *fcc* structure, while the 2θ of PtFeNi ZNWs shifts to higher angle than that of *fcc* Pt_3Fe, suggesting the formation of ternary alloys of Pt, Fe, and Ni. The Pt/Fe/Ni atomic ratio of the PtFeNi ZNWs is 52.3%/33.5%/14.2% (**Figure S2d**). The crystallinity and high-index facet-bounded surface of PtFeNi ZNWs were also confirmed by HRTEM (**Figure S2e**). The STEM-EDS elemental mappings of PtFeNi ZNWs show that the Pt, Fe, and Ni distribute evenly in the ZNWs (**Figure 2g**), confirming the alloyed structure of the PtFeNi ZNWs.

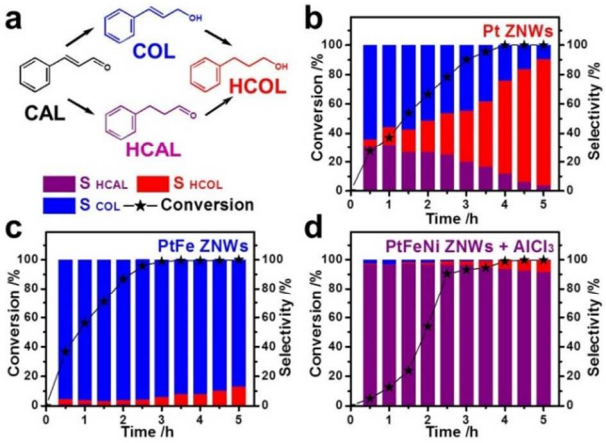

Figure 3. (a) Schematic CAL hydrogenation. CAL hydrogenation performances of (b) Pt ZNWs, (c) PtFe ZNWs, and (d) PtFeNi ZNWs+$AlCl_3$.

Table 1. Selective hydrogenation by Pt-based ZNWs catalysts.

Catalyst	Substrate	Tem. /°C	Time /h	Con. /%	Selectivity /%		
					UOL	SA	SOL
PtFe ZNWs (3.4 wt% Pt, ICP)	CAL	70	2.5	95.7	95.5	1.0	3.5
	CAL[a]	70	2	83.5	93.6	1.4	5.0
	CAL[b]	70	2	77.7	90.4	1.3	8.3
	Furfural	70	3.5	96.0	99.4	0.1	0.5
	Crotonaldetonalde-	40	4	88.3	80.3	2.4	17.3
	Guaiacene	70	5	92.7	90.0	1.3	8.7
PtFeNi ZNWs+ $AlCl_3$ (2.9 wt% Pt, ICP)	CAL	70	3.5	94.5	0.5	94.9	4.6
	CAL[a]	70	3	94.4	0.4	93.4	6.2
	CAL[b]	70	3	95.2	-	93.2	6.8
	Furfural	70	2.5	95.6	-	98.8	1.2
	Crotonaldetonalde-	40	1	99.5	-	99.9	0.1
	Guaiacene	70	1.5	99.0	0.3	97.7	1.0

[a] [b] Selective hydrogenation of the 1st and 5th reaction rounds.

To explore catalytic behaviour of these ZNWs for α, β-unsaturated aldehyde hydrogenation, we initially used CAL as a model molecule (**Figure S3**). The widely used and easily available TiO_2 was selected as support (**Figure S4**).[4] Firstly, CAL is hydrogenated to cinnamyl alcohol (COL) or hydrocinnamaldehyde (HCAL), and subsequently generated to hydrocinnamyl alcohol (HCOL) (**Figure 3a**). Pt ZNWs hy-

drogenate CAL at 70 °C and 0.1 MPa H_2 with selectivity for COL/HCAL/HCOL of 38.1%/16.8%/45.1% at the CAL conversion of 95.4% after 3.5 h (**Figure 3b&Table S1**). For comparison, the CAL conversion on Pt nanoparticles (NPs) and Pt NWs with smooth surface (**Figure S5**) is only 46.0% and 66.4% after 5 h with poor selectivity (**Figure S6a-b**). Considering that the CAL conversion of Pt ZNWs (95.4%) is 2.2 folds higher than that of Pt NWs (43.1%) after 3.5 h, the zigzag surface structure of Pt ZNWs significantly enhances hydrogenation activity. We further examined the catalytic properties of PtFe ZNWs and PtFeNi ZNWs (**Figure 3c&Figure S6c**). The PtFe ZNWs exhibit excellent COL selectivity (**Figure 3c**), with COL selectivity of 95.5% at 95.7% conversion after 2.5 h (**Table 1**). Furthermore, PtFeNi ZNWs exhibit similar selectivity as Pt ZNWs, but higher CAL hydrogenation activity (**Figure S6c**). To assess the intrinsic reactivity, turnover frequency (TOF) based on Pt was calculated.[1] The TOF of PtFeNi ZNWs (244.9 h^{-1}) is 2.8 and 2.5 folds higher than those of the Pt ZNWs (86.8 h^{-1}) and PtFe ZNWs (99.5 h^{-1}) (**Table S1**).

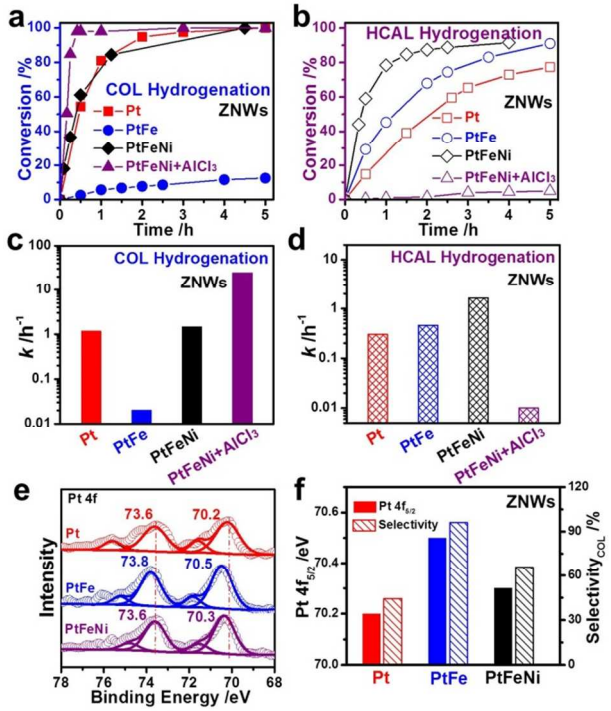

Figure 4. (a) COL and (b) HCAL hydrogenation performances of Pt ZNWs, PtFe ZNWs, PtFeNi ZNWs, and PtFeNi ZNWs+$AlCl_3$. The rate constant *k* values of (c) COL and (d) HCAL hydrogenation by Pt ZNWs, PtFe ZNWs, PtFeNi ZNWs, and PtFeNi ZNWs+$AlCl_3$. (e) Pt 4f XPS curves and (f) Pt $4f_{5/2}$ BEs and COL selectivity of different ZNWs.

Although thermodynamical favouring of the C=C hydrogenation over the C=O hydrogenation, Pt-based materials with high selectivity of C=C hydrogenation have been rarely reported.[7,29] Since the acid-base interaction between the Lewis acid and C=O can inhibit C=O hydrogenation to alcohol,[30] high selectivity of C=C group hydrogenation is expected to obtain by adding $AlCl_3$ as C=O protector. After adding Lewis acid, the performances of Pt ZNWs, PtFe ZNWs, and PtFeNi ZNWs for CAL hydrogenation were investigated (**Figure S7&Figure 3d**). CAL conversions on Pt ZNWs and PtFe ZNWs are below 5% after 5 h. However, PtFeNi ZNWs+$AlCl_3$ exhibit promising CAL hydrogenation behaviour, with the CAL conversion of 94.5%, HCAL selectivity of 94.9% after 3.5 h (**Table 1**). Indeed, the C=O stretching vibration (1692 cm^{-1}) peak disappears after adding $AlCl_3$ (**Figure S8**), which ensures the high selectivity of C=C hydrogenation.[30] Other Lewis acids can also achieve similar results (**Figure S7c-d**).

To find out why the high selectivity of C=O and C=C hydrogenation obtained by PtFe ZNWs and PtFeNi ZNWs+$AlCl_3$, the COL and HCAL hydrogenations were explored over Pt ZNWs, PtFe ZNWs, PtFeNi ZNWs, and PtFeNi ZNWs+$AlCl_3$ (**Figure 4a-b**). To better evaluate performances, the rate constant *k* was calculated from the rate equation $\ln(C/C_0) = kt$ (**Figure S9**). The ranking for *k* values of COL hydrogenation is PtFe ZNWs (0.02) << Pt ZNWs (1.16) < PtFeNi ZNWs (1.47) << PtFeNi ZNWs+$AlCl_3$ (24.78) (**Figure 4c&Table S2**). In contrast, the ranking for *k* values of HCAL hydrogenation is PtFeNi ZNWs+$AlCl_3$ (0.01) << Pt ZNWs (0.30) < PtFe ZNWs (0.46) < PtFeNi ZNWs (1.64) (**Figure 4d&Table S3**). The C=O hydrogenation *k* value ratio between PtFe ZNWs and Pt ZNWs is 1.5 and the *k* value ratio between C=O and C=C hydrogenation on PtFe ZNWs is 23.0, indicating that alloying Pt with Fe enhances C=O hydrogenation, meanwhile, deactivates the C=C hydrogenation. While the C=C hydrogenation *k* value ratio between PtFeNi ZNWs and PtFe ZNWs is 73.5 and the *k* value ratio between C=O and C=C hydrogenation on PtFeNi ZNWs+$AlCl_3$ is 4.0×10^{-4}, suggesting the synergism of PtFeNi ZNWs and $AlCl_3$ enhances the selectivity of C=C hydrogenation, in which PtFeNi ZNWs provide highly active sites and $AlCl_3$ is used as aldehyde protector (**Figure S10**).

Since surface atoms of catalysts have critical influence on the catalytic behaviour, the electronic properties of surface Pt were characterized by X-ray photoelectron spectroscopy (XPS) (**Figure 4e**). Pt 4f spectrum of Pt-based ZNWs clearly demonstrates that there are mainly Pt^0 with small portion of Pt^{2+} on the surface.[31,32] Compared with the binding energies (BE) of Pt^0 in Pt ZNWs (70.2 eV) and PtFeNi ZNWs (70.3 eV), the higher BE in PtFe ZNWs (70.5 eV) indicates the lower electron density of Pt, mainly caused by the electronic interaction between Fe and Pt. The variation tendency of both BE of Pt^0 and COL selectivity at ~ 50% conversion in Pt-based NWs is similar (**Figure 4f**), indicating that the lower electron density of surface Pt in PtFe ZNWs hinders the hydrogenation of C=C, consequently to high selectivity of C=O hydrogenation.[1]

To further study the universality, we used the optimized PtFe ZNWs and PtFeNi ZNWs+$AlCl_3$ to catalyze other α, β-unsaturated aldehyde hydrogenation (**Table 1&Figure S11**). Significantly, we found that PtFe ZNWs and PtFeNi ZNWs+$AlCl_3$ are generally highly active and selective for UOL and SA, respectively. For furfural hydrogenation, the furfuryl alcohol selectivity is 99.4 % at 96.0% conversion by using PtFe ZNWs (**Figure S11a**), whereas PtFeNi ZNWs+$AlCl_3$ exhibits high tetrahydrofurfural selectivity (98.8%) at 95.6% conversion (**Figure S11b**). Similar results are also obtained for crotonaldehyde (**Figure S11c-d**) and guaiacene (**Figure S11e-f**), where PtFe ZNWs and PtFeNi ZNWs+$AlCl_3$ generate high selectivity to the corresponding UOL and SA products. Moreover, stability of PtFe ZNWs and PtFeNi ZNWs+$AlCl_3$ was also explored. Both CAL conversion and selectivity for

COL and HCAL had limited changes after five reaction rounds (**Table 1&Figure S12**) and no noticeable differences in structure and surface property between fresh and used catalysts (**Figures S13-S15**).

To conclude, a series of Pt-based ZNWs were used as selective catalysts for α, β-unsaturated aldehyde hydrogenation. The excellent selectivities for UOL and SA were successfully realized by using the PtFe ZNWs and PtFeNi ZNWs+$AlCl_3$ as catalysts. The remarkable selectivity of PtFe ZNWs is attributable to the less electron density of Pt owing to electronic interaction between Fe and Pt, and PtFeNi ZNWs+$AlCl_3$ is due the high hydrogenation activity of PtFeNi ZNWs as well as the use of $AlCl_3$ as C=O protector to ensure the high selectivity of C=C hydrogenation. The present work highlights the importance of rational design of Pt-based NCs with precisely modulated structure and composition for catalysis and beyond.

ASSOCIATED CONTENT

Supporting Information

The Supporting Information is available free of charge on the ACS Publications website.

Experimental section, Figures S1–S15, and Tables S1–S3 (PDF)

AUTHOR INFORMATION

Corresponding Author

hxq006@suda.edu.cn

Notes

The authors declare no competing financial interests.

ACKNOWLEDGMENT

This work was financially supported by the Ministry of Science and Technology (2016YFA0204100, 2017YFA0208200), the National Natural Science Foundation of China (21571135), Young Thousand Talented Program, Jiangsu Province Natural Science Fund for Distinguished Young Scholars (BK20170003), and the Priority Academic Program Development of Jiangsu Higher Education Institutions (PAPD).

REFERENCES

(1) Zhao, M.; Yuan, K.; Wang, Y.; Li, G.; Guo, J.; Gu, L.; Hu, W.; Zhao, H.; Tang, Z. *Nature* **2016**, *539*, 76.
(2) Boudart, M. *Nature* **1994**, *372*, 320.
(3) Wu, B.; Huang, H.; Yang, J.; Zheng, N.; Fu, G. *Angew. Chem. Int. Ed.* **2012**, *51*, 3440.
(4) Kennedy, G.; Baker, L. R.; Somorjai, G. A. *Angew. Chem. Int. Ed.* **2014**, *53*, 3405.
(5) Loffreda, D.; Delbecq, F.; Vigné, F.; Sautet, P. *J. Am. Chem. Soc.* **2006**, *128*, 1316.
(6) Kahsar, K. R.; Schwartz, D. K.; Medlin, J. W. *J. Am. Chem. Soc.* **2014**, *136*, 520.
(7) Kliewer, C. J.; Bieri, M.; Somorjai, G. A. *J. Am. Chem. Soc.* **2009**, *131*, 9958.
(8) Liu, W.; Jiang, Y.; Dostert, K.; O'Brien, C. P.; Riedel, W.; Savara, A.; Schauermann, S.; Tkatchenko, A. *Sci. Adv.* **2017**, *3*, e1700939.
(9) Zhang, J.; Wang, L.; Shao, Y.; Wang, Y.; Gates, B. C.; Xiao, F. *Angew. Chem. Int. Ed.* **2017**, *56*, 9747.
(10) Song, S.; Liu, X.; Li, J.; Pan, J.; Wang, F.; Xing, Y.; Wang, X.; Liu, X.; Zhang, H. *Adv. Mater.* **2017**, 1700495.
(11) Tsang, S. C.; Cailuo, N.; Oduro, W.; Kong, A. T. S.; Clifton, L.; Yu, K. M. K.; Thiebaut, B.; Cookson, J.; Bishop, P. *ACS Nano* **2008**, *2*, 2547.
(12) Chen, S.; Su, H.; Wang, Y.; Wu, W.; Zeng, J. *Angew. Chem. Int. Ed.* **2015**, *54*, 108.
(13) Cao, S.; Tao, F.; Tang, Y.; Li, Y.; Yu, J. *Chem. Soc. Rev.* **2016**, *45*, 4747.
(14) Wang, Y.; Zhao, N.; Fang, B.; Li, H.; Bi, X. T.; Wang, H. *Chem. Rev.* **2015**, *115*, 3433.
(15) Zhang, Z.; Liao, H.; Gong, Y.; Gu, L.; Qu, X.; You, L.; Liu, S.; Huang, L.; Tian, X.; Huang, R.; Zhu, F.; Liu, T.; Jiang, Y.; Zhou, Z.; Sun, S. *Nano Energy* **2016**, *19*, 198.
(16) Ye, W.; Chen, S.; Ye, M.; Ren, C.; Ma, J.; Long, R.; Wang, C.; Yang, J.; Song, L.; Xiong, Y. *Nano Energy* **2017**, *39*, 532.
(17) Zhao, X.; Chen, S.; Fang, Z.; Ding, J.; Sang, W.; Wang, Y.; Zhao, J.; Peng, Z.; Zeng, J. *J. Am. Chem. Soc.* **2015**, *137*, 2804.
(18) Stamenkovic, V.; Mun, B. S.; Mayrhofer, K. J. J.; Ros, P. N.; Markovic, N. M.; Rossmeisl, J.; Greeley, J.; Nørskov, J. K. *Angew. Chem. Int. Ed.* **2006**, *45*, 2897.
(19) Yu, W.; Porosoff, M. D.; Chen, J. G. *Chem. Rev.* **2012**, *112*, 5780.
(20) Rodriguez, J. A.; Goodman, D. W. *Science* **1992**, *257*, 897.
(21) Fleischer, S.; Zhou, S.; Junge, K.; Beller, M. *Angew. Chem. Int. Ed.* **2013**, *52*, 5120.
(22) Yang, J. W.; Hechavarria, F. M. T.; Vignola, N.; List, B. *Angew. Chem. Int. Ed.* **2004**, *44*, 108.
(23) Loffreda, D.; Delbecq, F.; Vigné, F.; Sautet, P. *Angew. Chem. Int. Ed.* **2005**, *44*, 5279.
(24) Murillo, L. E.; Goda, A. M.; Chen, J. G. *J. Am. Chem. Soc.* **2007**, *129*, 7101.
(25) Bu, L.; Ding, J.; Guo, S.; Zhang, X.; Su, D.; Zhu, X.; Yao, J.; Guo, J.; Lu, G.; Huang, X. *Adv. Mater.* **2015**, *27*, 7204.
(26) Bu, L.; Guo, S.; Zhang, X.; Shen, X.; Su, D.; Lu, G.; Zhu, X.; Yao, J.; Guo, J.; Huang, X. *Nat. Commun.* **2016**, *7*, 11850.
(27) Tian, N.; Zhou, Z.; Sun, S.; Ding, Y.; Wang, Z. L. *Science* **2007**, *316*, 732.
(28) Wu, H.; Chen, O.; Zhuang, J.; Lynch, J.; LaMontagne, D.; Nagaoka, Y.; Cao, Y. C. *J. Am. Chem. Soc.* **2011**, *133*, 14327.
(29) Dostert, K.; O'Brien, C. P.; Ivars-Barceló, F.; Schauermann, S.; Freund, H. *J. Am. Chem. Soc.* **2015**, *137*, 13496.
(30) Liu, H.; Jiang, T.; Han, B.; Liang, S.; Zhou, Y. *Science* **2009**, *326*, 1250.
(31) Chen, C.; Kang, Y.; Huo, Z.; Zhu, Z.; Huang, W.; Xin, H. L.; Snyder, J. D.; Li, D.; Herron, J. A.; Mavrikakis, M.; Chi, M.; More, K. L.; Li, Y.; Markovic, N. M.; Somorjai, G. A.; Yang, P.; Stamenkovic, V. R. *Science* **2014**, *343*, 1339.
(32) Stassi, J. P.; Zgolicz, P. D.; Miguel, S. R.; Scelza, O. A. *J. Catal.* **2013**, *306*, 11.

TOC Graphic

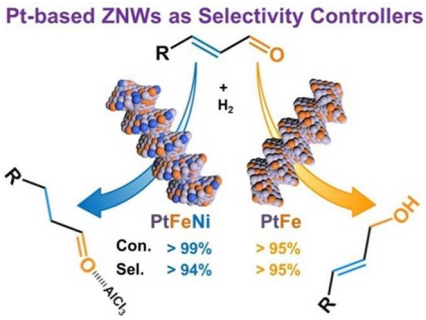
Pt-based ZNWs as Selectivity Controllers
R
O
+
H2
PtFeNi
PtFe
Con. > 99% > 95%
Sel. > 94% > 95%
OH
R
R
O
AlCl3